

Laser Micro-Patterning by Means of Optical Fibers with Micro-grinded Lens End Faces

S. Yakunin, J. Heitz

Institute of Applied Physics, Johannes Kepler University Linz, A-4040 Linz, Austria

E-mail: sergii.yakunin@jku.at

We report on laser micro-patterning of polymer surfaces using lensed optical fibers with a distance of a few μm to the surface. For control of the fiber tip position and tip-to-sample distance, we used a scanning probe microscopy (SPM) setup. This setup can also be employed as atomic force microscope (AFM) with the fiber tip as AFM probe. Additional, the SPM setup was used for production of the lensed fibers by polishing. Structures in the order of 100 nm cross-section could be obtained a micro-grinded lens end fiber with a tip-to-sample distance of 1 μm , which corresponded to focal length of the fiber lens.

DOI:10.2961/jlmn.2011.03.0001

Keywords: laser, direct writing, polymer, near-field, AFM, lensed fibers.

1. Introduction

Nano-patterning of polymer surface has found a wide range of applications including biotechnology, where holes in the size of hundreds – nm can influence the growth and differentiation of relatively large living cells [1]. Instead of the e-beam patterning technique used in the Ref. 1, we applied direct writing by laser-light. In our previous papers [2,3], we have demonstrated that this technique allows the production of sub-wavelength structures in the optical near field of a fiber tip. In conventional scanning near-field optical microscopy (SNOM), the light is confined to a sub-wavelength region in the near-field of a drawn metal coated optical fiber tip [4]. In the last years, SNOM setups with uncoated etched fibers were employed for laser-induced process on micrometer or nanometer scale, i.e., for photochemical etching [2, 3] and even for laser ablation [5] with plasma spectral analysis [6,7]. These applications need rather high pulsed laser intensities, which can be hardly transferred through etched tips due to their relatively low transmission efficiency [8]. Additionally, the light intensity drastically decreases with increasing distance between sample surface and tip due to the high divergence of the point-like light source formed by the fiber tip.

Another approach for tight light focusing is the use of high numerical aperture (NA) micro optics such as microspheres [9] and microlenses [10]. Monolayers of quartz microspheres allow to focus the light to a hexagonal array of spots with a size well below the wavelength of light [11]. The amount of light transferred to the focused spot is comparable with usual optics. But addressing of the light to a concrete position is difficult, because it requires a precise manipulation of the individual microsphere or microlens.

It should be possible to combine the advantages of these two approaches in a scanning probe microscope setup by means of lensed fiber tips. This allows a relative simple positioning together with high transmission efficiency. The concept of lensed fibers was suggested for laser diode irradiation coupling already about three decades ago [12,13]. Recently, this technique found new applications, but the

production procedures of lensed fibers have still a large improvement potential [14-16]. The most precise commercially available lensed fibers of spherical shape are limited to the radius of curvature above 3 - 5 μm . Micro-precision fabrication techniques (like ion-milling) seem to be feasible, but rather time consuming and expensive.

In [17,18], we proposed a novel method of lensed fibers grinding for fabrication of lensed fibers with a smaller radius of curvature than commercially available. This method offers also a high degree of versatility regarding tip shape, but is still rather simple in comparison to micro-fabrication techniques like ion-milling. This micro-grinding technique uses a fixed fiber that differs from procedures, where the fiber is rotated in contact with the grinding surface. In our case, the rotation movement of the fiber is replaced by a lateral concentric movement inside a polishing surface of conical shape. The stable position of the fiber allows us to employ a shear-force tip-sample distance controller similar as in a typical non-contact mode AFM. An additional advantage is that this method allows to grind fibers without a limitation in total fiber length that was impossible for the rotation setups.

We used the scanning probe microscope for tip grinding as well as for the characterization of the obtained lensed fibers with two complementary techniques: topography measurement in AFM mode and intensity distribution measurement of the light passing through the fiber in SNOM mode. We grinded several samples of single- and multimode fiber tips and characterized their topography and optical properties. The obtained lensed fibers have the potential for wavelength and sub-wavelength spot size focusing. In preliminary experiments, we demonstrated the use of lensed fibers tip for chemical material analysis in laser-induced breakdown spectroscopy (LIBS) [19]. The use of the lensed fiber reduced the pulse energy needed for plasma ignition and allows to operate the system with a certain tip-to-samples distance, which is favorable for durability. In the present work, we put the special focus on

procedure for patterning of polymer surface through the lensed fibers.

2. Experimental

The experiments were performed with 250 μm thick step index quartz multimode fibers with a numerical aperture NA of 0.22 (laser Components, type 2524002). The fibers were first chemically etched to a conical shape and then grinded to a hemispherical shaped lens with curvature radii of 1 - 3 μm .

The setup for direct writing and lensed fiber grinding is based on a home-made AFM/SNOM and described in details in [7]. The main changes that transform scanning system of the SNOM to a micro-grinding station are the software algorithms for tip trajectory control. Additionally, we modified the electronic part of the feedback loop by introduction of an optional modulation in Z-axis direction by means of an external periodical driver. The setup is schematically depicted in Fig. 1.

- a step-height etalon (4b) with square holes in the AFM operation-mode;
- a pinhole (4c) with a photodiode (6) behind it in the SNOM operation-mode.
- a thin polymer layer (4d) in mode of patterning.

The polishing surface is made from an aluminum oxide fine polishing sheet with a grain size of 0.3 μm (Thorlabs). To obtain the conical indentation, we pressed metal pins with calibrated cone angles into the polishing sheet. The resulting topography of the conical indentation is shown as inset 4a in Fig.1. The image was measured with an etched fiber in the same setup in the AFM operation-mode. The shape of the indentation is used for the determination of the grinding trajectory.

We used a standard etalon (Veeco, SHSPT-200-CP) as test sample for the characterization of the AFM tip topography. This etalon consists of an array of equal 5 \times 5 μm square holes with a depth of 200 nm. The feature 4b of Fig. 1 shows a 3D AFM image of the step-height etalon

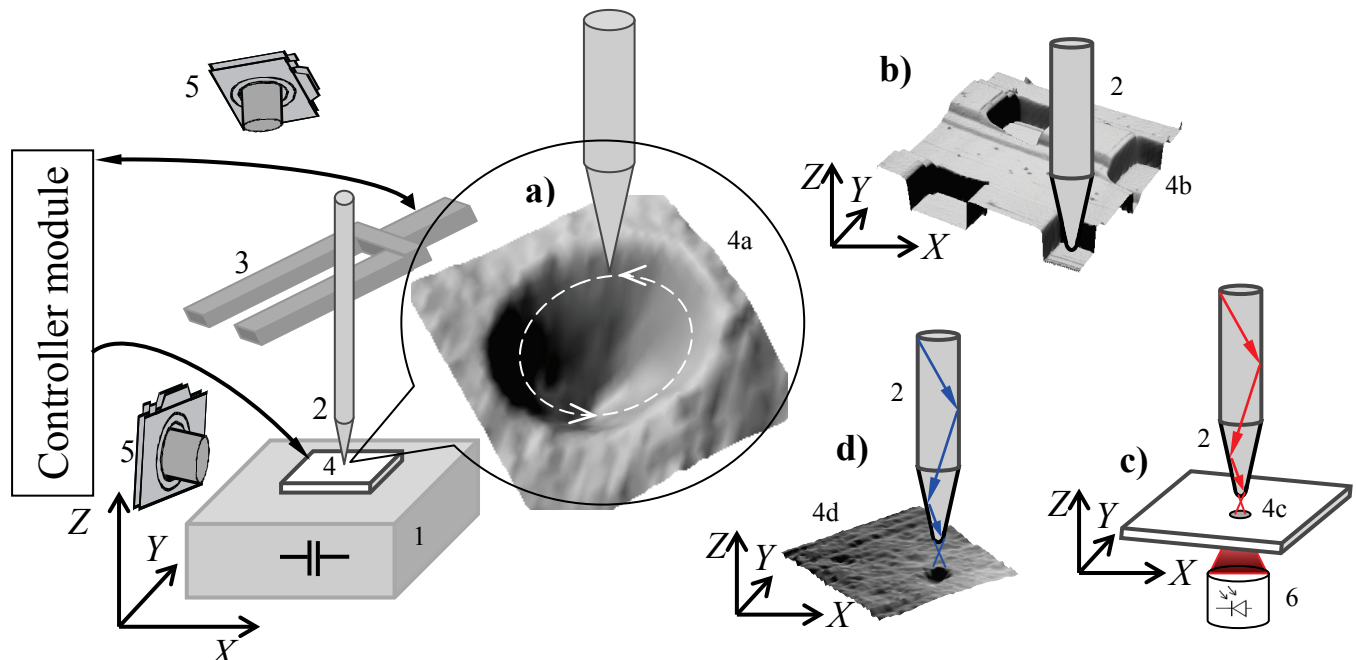


Fig. 1 Micro-grinding AFM/SNOM setup. 1 – nano-positioning stage, 2 – optical fiber tip, 3 – tuning fork, 4 – sample (4a – polishing paper, 4b – AFM etalon, 4c – pinhole , 4d – polymer layer), 5 – digital microscopes, 6 – photodiode.

The scanning system is a 1500 \times 1500 \times 250 μm XYZ piezo-electric translation stage (1). Additionally, a manual translation stage is included in the fiber head for rough positioning. The distance sensor consists of the fiber tip (2), which is mechanically pressed to a quartz tuning fork (3), and the electronic signal of the fork oscillation, which is used for the feedback loop of the Z piezo-electric stage. The XY coordinates are controlled by a computer by means of internal capacitor sensors in the piezo-electric stages. The piezo-electric stage fixes rigidly the sample (4) that is in contact with the fiber tip. Depending on the mode of operation, the sample can be

- a polishing surface with a conical indentation (4a) in the operation-mode of grinding;

recorded with a commercial Veeco CP-II AFM in contact mode.

For the beam intensity map measurements, we employed a commercial pinhole (Newport, PH-1.0) with an aperture diameter of 1 μm in a molybdenum foil of 13 μm thickness. The pinhole and the photo-diode behind it are schematically shown as features 4c and 6 of Fig.1, respectively.

As sample we used PMMA (Goodfellow) sheets as well as PMMA thin films (thickness 1 - 3 μm) spin-coated at polished glass substrates from chloroform solution [20] with subsequent drying at a temperature of 120 °C for 2 hours.

For the patterning, we used the continuous-wave radiation of a quadrupled Nd:YAG diode-pumped solid-state laser. The resulting laser beam with 266 nm wavelength is produced by sequential frequency doubling: initially by an intra-cavity process inside the laser source (Coherent, Verdi V-5) and then by with the external unit MBD-266. The laser beam with a diameter about 2 mm was focused by a quartz lens with a focal length of 90 mm to the flat-polished end of the optical fiber with a length of about 2 m. The laser power was measured before the coupling lens. We roughly estimate the total losses for coupling and delivery 60 - 70%.

3. Results and Discussion

In a first process step, the fibers were chemically etched to conical tips in 40% HF aqueous solution like in ref. [21]. Then we produced the lensed shape of fiber tips by grinding inside the conical indentation in the polishing surface. The feature 4a shows an 3D AFM image of an indentation recorded with our setup in the AFM operation mode with a freshly etched tip. The trace with arrows shows schematically the trajectory of the relative movement of the tip inside the indentation during the grinding procedure. The trajectory is a circle in the horizontal plane with the center at the indentation axis. The radius and XYZ circle centre coordinates are adaptively adjusted during the grinding process to provide constant contact of the tip to polishing surface at all trajectory points.

The production procedure for a hemispherical tip shape consists of two steps. In the first step, the initially conical tip is truncated. This polishing step is performed at a flat surface without indentation. The procedure doesn't require special care on an optimal trajectory. I.e., we used a Lissajous curve that resembles the number 8. It is only important to limit the pressing force between tip and polishing paper at the initial stage of grinding to avoid tip crumbling. After an initial stage, the grinding rate was increased by an additional vertical oscillation movement with a frequency of 200 Hz and an amplitude of 0.1 to 0.5 μm by means of a sinusoidal signal from functional generator added to the feedback loop. In the second step of the polishing procedure, we grinded the truncated tip in the indentation with an appropriate slope angle and depth. Again, we added a Z-oscillation with an amplitude up to 1 μm . In most cases, the combination of two polishing steps it was enough to achieve a satisfactory result. Due to minor distortions at the polishing surface and variations of trajectory movement, the resulting tip shape is rather smooth. However, it is also possible to apply more grinding steps with different slope angles.

For tip topography measurement, we used the effect that the resulting AFM cross-sections are blurred due to convolution with the tip geometry [22] (color lines in Fig. 2)). It is possible to restore the real probe shape from the recorded image of the etalon with known topography shape by a deconvolution method described in [23]. The etalon is sufficiently sharp to provide only a single point of contact to the tip during scanning which is a requirement for the successful tip shape reconstruction. For the case of a sharp

step profile (as for the etalon, black line in Fig. 2), the deconvolution process is rather simple and described in details in [18].

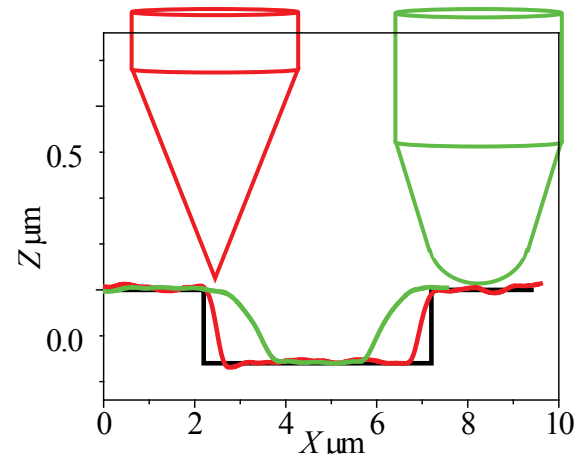


Fig. 2 AFM etalon profile (black), profiles recorded by the probes of corresponding color (red and green lines).

In our case, this deconvolution method is quite effective as the tip shape measurement can be performed directly in the polishing setup without extraction of the tip. For this, the polishing surface and the etalon have to be mounted on the same sample holder.

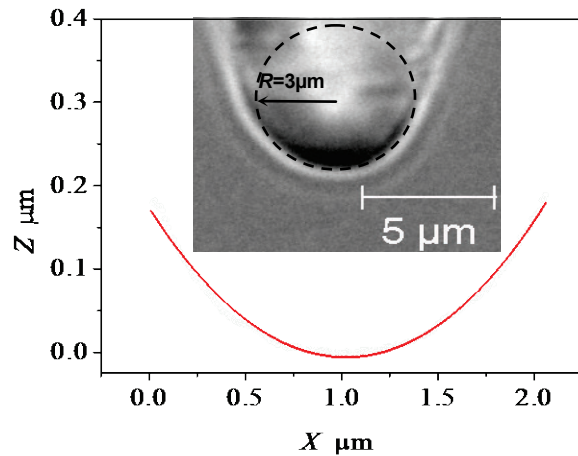


Fig. 3 Tip profile restored by deconvolution: dots - experimental data, solid line – fit with the model of a spherical tip shape. In the inset, we show a microscopic image of the same tip together with circle of radius $R = 3 \mu\text{m}$ (dashed line).

Fig. 3 shows the reconstructed AFM topography profile (dots) with a lateral resolution of 10 nm and in comparison to a circle function with radius $R = 3 \pm 0.05 \mu\text{m}$ obtained by fitting (red solid line). The orthogonal Y cross-section gives a similar result. The etalon hole depth is 200 nm. Therefore, the tip topography is limited to this value in Z direction. As can be seen in the microscopic image in the

inset to Fig. 3, the fiber tip shape is rather good described as part of a spherical surface with a radius of 3 μm , which is in good agreement with the AFM topography estimation.

To assess of the light focusing abilities of the lensed fibers, we analyzed the light intensity distribution in the near- and far-field of the tip by means of a scanning pinhole. For this measurement, we coupled a cw He-Ne laser into the fiber and scanned the pin hole (feature 4c in Fig.1) layer-by-layer at distances Z between tip and pinhole plane ranging from 0.1 to 10 μm . The light intensity measurement itself was performed by a sensitive photodiode behind the pinhole.

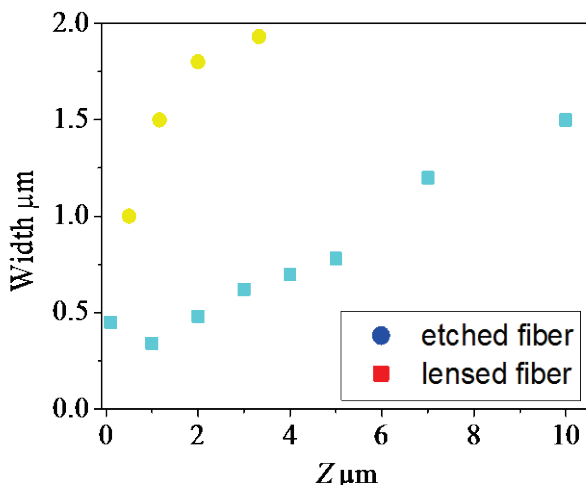


Fig. 4 Width (FWHM) of beam profile as function of the tip-to-pinhole distance Z for different tip geometries: grinded hemispherical tip (squares), chemically etched tip (circles).

Figure 4 shows the width of the beam profile (full width at half maximum, FWHM) as function of the tip-to-pinhole distance for a hemispherical lensed tip at a multimode step-index fiber and a chemically etched tip without polishing. The values of FWHM were derived from the intensity recorded for the various distances. The results for the hemispherical lensed fiber (squares in Fig. 4) show an effective focusing at a distance about one micrometer. The FWHM diameter value of about 340 nm at the waist is about half of the light wavelength 632 nm. It could be even smaller because of the limited lateral resolution due to the finite size of the pinhole, which leads to a broadening of the beam profile. Farther from the waist position, the beam diverges linearly, similar as expected for a Gaussian mode. The distance dependence of FWHM is shown as well for a conical single-mode fiber tip that was chemically etched with cone angle of about 15° (circles in Fig. 4). We were not able to record the real FWHM value in direct contact with the etched tip due to the rather wide pinhole diameter. Consistently with previous results in refs. [2,3], we suggest that it is much smaller than 0.5 μm , which is the FWHM value measured for the lensed tip in contact. At larger distances, the emitted beam of the etched fiber diverges fast.

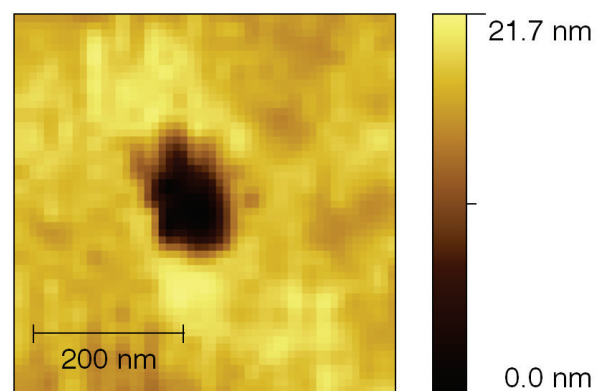


Fig. 5 AFM topography of PMMA patterned by lensed fiber.

Figure 5 shows an AFM image of a nano-structure in PMMA produced by cw 266 nm laser irradiation by mean of a lensed optical fiber with a radius of curvature of about 3 μm and a tip-to-sample distance of about 1 μm . The irradiation time was 1 s and the laser power before coupling was about 50 mW. We want to point out that the AFM image is recorded with the same fiber tip as used for patterning by operating the SPM setup in the AFM mode. Therefore the lateral resolution of the image is worse than in usual commercial AFM. However, to perform the patterning and the characterization may provide advantages for many applications. The cross-section of the nano-structure in Fig. 5 is about 150 nm (FWHM). The minimal feature cross-sections reached by these technique with lensed fibers in PMMA was about 80 nm so far. With sharp conical etched fiber tip in contact mode, we reached in PMMA feature sizes with about 60 nm. However, in contact mode there is a thermo-mechanical contact and the heated polymer surface. This can result in scratches by relative tip movement due thermal expansion, material deposition at the tip surface and in tip degradation by mechanical wear. All these effects are much less pronounced when using lensed fiber tips due to the distinct tip-to-sample distance. The achieved dimensions of the nano-structures are comparable to those in ref. [1], which are employed there for influencing the growth and differentiation of biological cells seeded at the nano-patterned surface. In the future, we want to perform similar experiments with laser-induced nano-patterns as those described above.

4. Conclusion

We adapted a home-made scanning probe setup for micro-grinding of lensed fibers from chemically etched tips to predefined shapes with radii down to the sub-micron range. In the same setup, it is possible to perform a tip quality characterization by AFM or SNOM type measurements. We performed direct patterning of PMMA surfaces by UV laser irradiation through optical fibers with micro-grinded lens end faces. Produced features are slightly larger than features patterned with sharp conical etched fiber tips in contact mode. But the main advantage in the used of lensed fibers is the absence of the direct contact between tip and sample surface. This eliminates mostly mechanical damage

of the tip and therefore can probably increase the tip durability time and allow increased writing speeds.

Acknowledgments

The Austrian NANO Initiative is acknowledged for financial support under the project NSI_NBPF.

References

- [1] M.J. Dalby, N. Gadegaard, R. Tare, A. Andar, et.al.: Nat Mater., 6, (2007) 997.
- [2] G. Wysocki, S.T. Dai, T. Brandstetter, J. Heitz, and D. Bäuerle: Appl. Phys. Lett., 79, (2001) 159.
- [3] G. Wysocki, J. Heitz, and D. Bäuerle: Appl. Phys. Lett., 84, (2004) 2025.
- [4] Y. Inouye and S. Kawata: Opt. Lett., 19, (1994) 159.
- [5] D. J. Hwang, H. Jeon, and C. P. Grigoropoulos: Appl. Phys. Lett., 91, (2007) 251118-1.
- [6] D. J. Hwang, H. Jeon, C. P. Grigoropoulos, J. Yoo, and R. E. Russo: J. Appl. Phys., 104, (2008) 013110-1.
- [7] J. Heitz, S. Yakunin, T. Stehrer, G. Wysocki, and D. Bäuerle: SPIE Proc., 7131, (2009) 71311W.
- [8] P. Moar, F. Ladouceur, and L. Cahill: Appl. Opt., 39, (2000) 1966.
- [9] E. Mcleod and C. B. Arnold: Nature Nanotechnology, 3, (2008) 413.
- [10] Ju. Y. Lee, B. H. Hong, W. Y. Kim, et.al.: Nature, 460, (2009) 498.
- [11] D. Brodoceanu, L. Landström, and D. Bäuerle: Appl. Phys., A 86, (2007) 313.
- [12] H. Sakaguchi, N. Seki, and S. Yamamoto: Electron. Lett., 17, (1981) 425.
- [13] M. Kawachi and T. Edahiro: Electron. Lett., 18, (1982) 71.
- [14] Y.-T. Tseng, T.-Y. Hung, J.-H. Liu, and C.-H. Chang: Int. J. Mach. Tool Manu., 47, (2007) 892.
- [15] S. Lin: Precision engineering, 29, (2005) 146.
- [16] T. Grosjean, S. S. Saleh, M. A. Suarez, et.al.: Applied Optics, 46, (2007) 8061.
- [17] S. Yakunin, J. Heitz, and T. Stehrer: Austrian patent application AT869/2009.
- [18] S. Yakunin, J. Heitz: Applied Optics, 48, (2009) 6172.
- [19] S. Yakunin, T. Stehrer, J. D. Pedarnig, and J. Heitz: J. Optoelectr. Adv. Mat., 12, (2010) 758.
- [20] N.G. Semaltianos: Microelectronics Journal, 38, (2007) 754.
- [21] R. Stockle, C. Fokas, V. Deckert, et.al.: Appl. Phys. Lett., 75, (1999) 160.
- [22] P. M. Williams, K. M. Shakesheff, M. C. Davies et.al.: J. Vac. Sci. Technol., B 14, (1996) 1557.
- [23] A. A. Bukharaev, N. V. Berdunov, D. V. Ovchinikov, and K. M. Salikhov: Scanning Microscopy, 12, (1998) 225.

(Received: June 07, 2010, Accepted: October 10, 2011)